Journal of Medicinal Chemistry

ARTICLE

pubs.acs.org/jmc

Synthesis, Characterization, and in Vivo Delivery of siRNA-Squalene Nanoparticles Targeting Fusion Oncogene in Papillary Thyroid Carcinoma

Mouna Raouane,[†,‡,§] Didier Desmaele,[†] Marie Gilbert-Sirieix,[‡] Claire Gueutin,[†] Fatima Zouhiri,[†] Claudie Bourgaux,[†] Elise Lepeltier,[†] Ruxandra Gref,[†] Ridha Ben Salah,[§] Gary Clayman,[∥] Liliane Massaad-Massade,*[,‡] and Patrick Couvreur*[,†]

[†]Laboratoire de Physicochimie, Pharmacotechnie et Biopharmacie, Faculté de Pharmacie, UMR CNRS 8612, Université Paris Sud 11, 5 Rue J. B. Clément, 92296 Châtenay-Malabry, France

[‡]Laboratoire de Vectorologie et Transfert de Gènes, UMR CNRS 8203, Institut Gustave Roussy, 114 Rue Edouard Vaillant, 94805 Villejuif, France

[§]Unité de Recherche de Biophysique, 00/UR/08-02, Faculté de Médecine Ibn El Jazzar de Sousse, Université de Sousse, Avenue Mohamed Karoui, 4002 Sousse, Tunisia

[∥]Department of Head and Neck Surgery, The University of Texas MD Anderson Cancer Center, Houston, Texas 77030, United States

Supporting Information

ABSTRACT: We report the conjugation of the natural lipid squalene (SQ) with a small interfering RNA (siRNA), against the junction oncogene RET/PTC1, usually found in papillary thyroid carcinoma (PTC). The acyclic isoprenoid chain of squalene has been covalently coupled with siRNA RET/PTC1 at the 3′-terminus of the sense strand via maleimide−sulfhydryl chemistry. Remarkably, the linkage of siRNA RET/PTC1 to squalene led to an amphiphilic molecule that self-organized in H_2O as siRNA-SQ RET/PTC1 nanoparticles (NPs). The siRNA-SQ RET/PTC1 NPs, stable in H_2O, were used for biological studies. In vitro, they did not show any cytotoxicity. Interestingly, in vivo, on a mice xenografted RET/PTC1 experimental model, RET/PTC1-SQ NPs were found to inhibit tumor growth and RET/PTC1 oncogene and oncoprotein expression after 2.5 mg/kg cumulative dose intravenous injections. In conclusion, these results showed that the "squalenoylation" offers a new noncationic plate-form for the siRNA delivery.

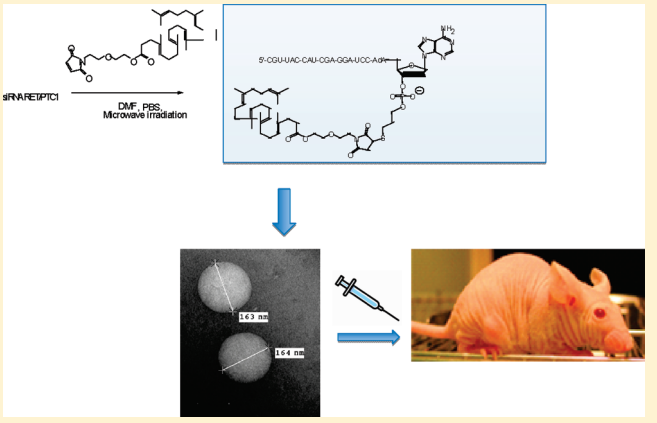

INTRODUCTION

Among all thyroid cancers, the papillary thyroid carcinoma (PTC)[1] is the most frequent.[2] It is associated with somatic mutations of the *RET* proto-oncogene encoding for a membrane tyrosine kinase (TK) receptor that is normally not expressed in the thyroid follicular cells. The most common variant is RET/PTC1 which is formed by an intrachromosomic rearrangement, leading to the juxtaposition of the RET TK domain with the genes H4.[3−5] RET/PTC1 fusion oncogene occurred in children after the nuclear fallout in the Chernobyl area[6] and after external irradiation to medical treatment.[7,8]

The prognosis of PTC is generally good, but a considerable number of patients, approximately 30% as shown after 30 years of follow-up, have recurrent disease. This constitutes, therefore, an area of important research on emerging therapies such as using small interfering RNA (siRNA) for targeting the *RET/PTC1* fusion oncogene and inducing the silencing of the corresponding protein. Such therapeutic approach is highly specific because RET/PTC1 is present only in the tumor cells and not in the surrounding normal cells. Recently, a siRNA RET/PTC1 efficient and specific to *RET/PTC1* oncogene has been discovered; this opens new prospects in the treatment by siRNAs of PTC with *RET/PTC1* junction.[9] However, in vivo delivery of siRNA is a key challenge because the biological efficacy of the siRNAs is hampered by their poor stability in biological fluids and low intracellular penetration due to their highly hydrophilic and anionic character.[10,11]

So far, a wide variety of approaches including viral vectors and nonviral delivery systems, such as liposomes, nanoparticles, micelles, and polyplexes,[12−14] have been investigated to enhance target cells uptake and silence potency in vivo. However, the

Received: January 17, 2011
Published: May 11, 2011

dx.doi.org/10.1021/jm2000272 | *J. Med. Chem.* 2011, 54, 4067–4076

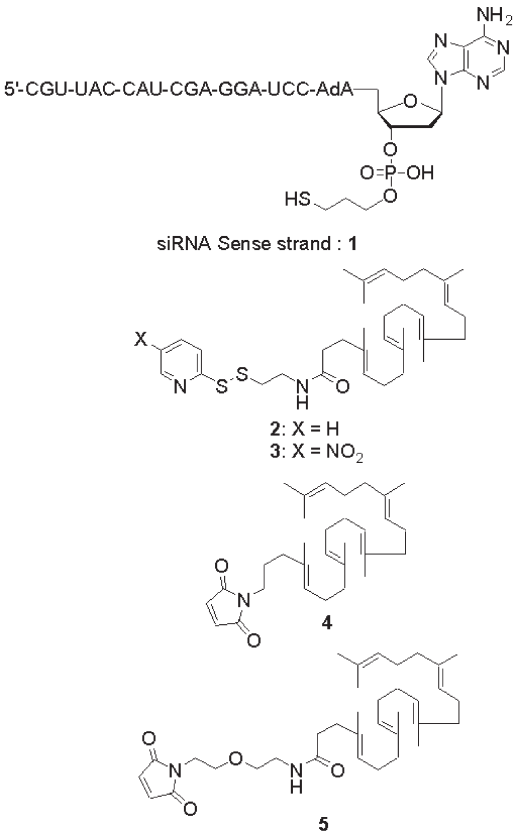

Figure 1. Chemical structure of the siRNA sense strand **1** and of the squalenoyl activated moieties **2**−**5**.

safety of viral vectors is questionable because of immunogenicity and possible recombination of oncogenes. On the other hand, most of the nonviral vectors are designed using polycations, either polymers or lipids, whose (cyto)toxicity is now well documented.[15,16] This is the reason why the conjugation of nucleic acids with neutral lipids offers an interesting alternative. Thus, DNA-programmed lipids, consisting of two 18-carbon alkyl hydrophobic tails linked covalently to the 5′-termini of a 9-mer single stranded DNA, have been proposed as responsive liposomes.[17] In another interesting approach, a simple lipid tail phosphoramidite with diacyl chains has been attached onto the end of an aptamer via a polyethylene glycol linker to obtain self-assembled micelles able to target cancer cells.[18] Different types of cholesterol-conjugated siRNA were also synthesized to elucidate the requirements for siRNA delivery in vivo. However, the pharmacological efficacy of these approaches remains to be demonstrated in experimental pathologies.[19] Noteworthy, the in vitro demonstration that alkyne-modified lipids derived from cholesterol and covalently conjugated to azido oligonucleotides could efficiently inhibit hepatitis C virus translation in human hepatic cells has been done by the group of Barthelemy.[20] Thus, although further in vivo efficacy is needed, amphiphilic oligonucleotides may represent an interesting marriage of nucleic acids with lipids.[21] In this context, we introduce here the idea to covalently link siRNA with the squalene, a natural and nonionic lipid. This triterpene is known for its dietary benefits,[22] biocompatibility, and inertness so that it is already extensively used as excipient in numerous pharmaceutical formulations for oral and parenteral administration.[23] From a safety point of view, this lipid

Scheme 1. Synthesis of Squalenoyl Maleimide 5 and Conjugate Addition of the Sense Strand siRNA 1 with 5 To Give RET/PTC1 siRNA-SQ (9)

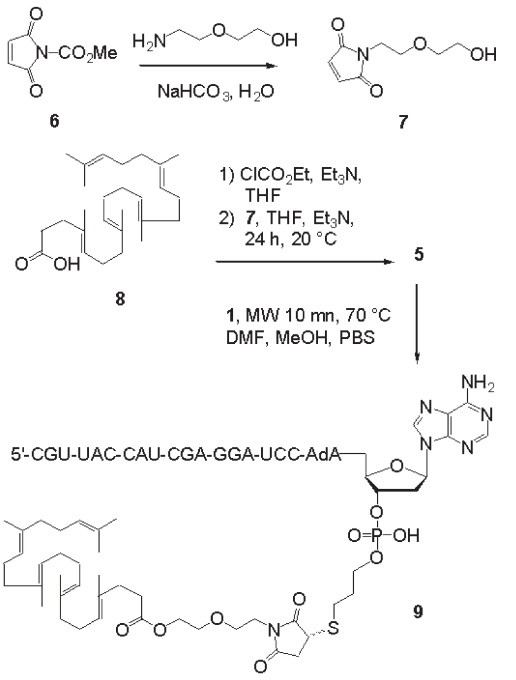

is therefore more desirable than cholesterol and fatty acid, of which intravenous administration may be linked with cardiovascular events. Thus, in the present study, we propose to conjugate RET/PTC1 siRNA to squalene in order to improve siRNA hydrophobicity and stability and to demonstrate the efficacy of this treatment on a mice xenografted RET/PTC1-expressing tumor. The concept to chemically link the squalene to a biologically active drug molecule in order to create a bioconjugate, which can self-aggregate as nanoassemblies in water, has already been demonstrated using (mono)nucleosides analogues with anticancer (e.g., gemcitabine in leukemic cancer) or antiviral activity (ddC).[24] Interestingly, the gemcitabine−squalene nanoassemblies were able to deliver this drug efficiently into the cell cytoplasm through a nonendocytotic pathway, thus bypassing lysosomal degradation.[25] This is another reason why we have extended this strategy here to siRNA RET/PTC1 oligonucleotides (ONs).

CHEMISTRY

One of the critical problems in RNA-based therapeutic applications is the delivery of intact siRNA across plasma membranes of cells. In the present study, we have designed a new squalene−siRNA bioconjugate to protect siRNA from degradation and to improve the cell delivery by increasing the overall lipophilicity of the nucleic acid derivative. In order to protect the siRNA RET/PTC1 against 3′-exonucleases, simultaneously preventing steric hindrance toward recognition of the targeted mRNA by the antisense strand and also allowing fixation of proteic RISC complex at the 5′-end (that requires phosphorylation), we directly linked squalene at the 3′-end of the 21-mer sense strand siRNA **1** (Figure 1). This coupling strategy was based on previous studies showing that the modification of the 5′-hydroxyl groups of the guide siRNA strand by methoxy groups completely hampered the siRNAs function in

dx.doi.org/10.1021/jm2000272 |J. Med. Chem. 2011, 54, 4067–4076

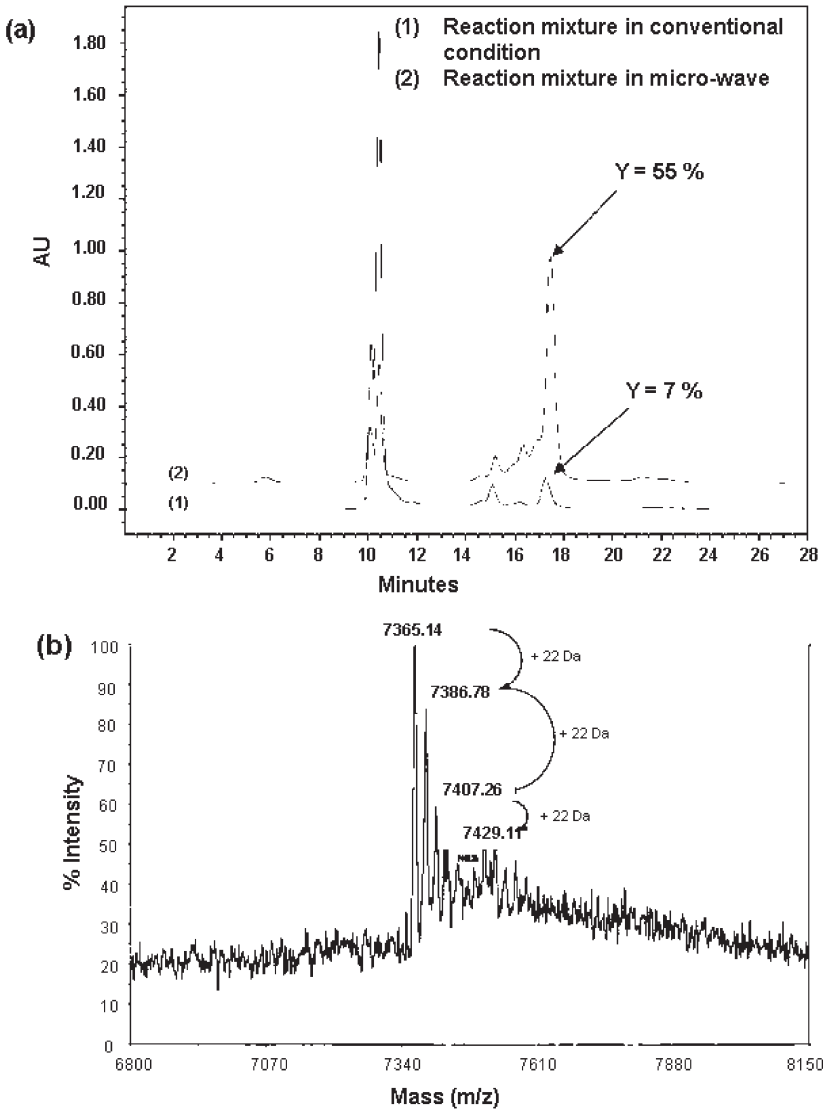

Figure 2. Characterization of RET/PTC1 siRNA-SQ sense strand bioconjugate. (a) HPLC profile of reaction mixture. Arrows show the elution peal of RET/PTC1 siRNA bioconjugate. Significant increase in the reaction yield (from 7% to 55%) was observed when 30% methanol was added to the reaction mixture as a cosolvent and when reaction activation was performed by microwave irradiation. Chromatogram 1 corresponds to the reaction mixture obtained in conventional heating conditions. Chromatogram 2 corresponds to the reaction mixture obtained in the presence of 30% methanol and reaction activation by microwave irradiation. (b) MALDI-TOF mass spectrometry analysis of the RP-HPLC purified RET/PTC1 siRNA-SQ sense strand bioconjugate. The MALDI-TOF mass spectrum shows a bioconjugate molecular weight of 7365.14 Da in agreement with the calculated molecular weight.

Table 1. RP-HPLC Elution Times of RET/PTC1 siRNA-SQ versus RET/PTC1 siRNA

compd	elution time (min)
CGU UAC CAU CGA GGA UCC AAA	10.5
CGU UAC CAU CGA GGA UCC AAA SQ	17.5

Drosophila embryo lysate and HeLa cell extract.[29,30] At the outset of this study, we chose to link covalently the siRNA sense strand **1** to squalene through a disulfide linkage, taking advantage of the 3-mercaptopropyl phosphate group introduced at the 3′-terminal of the oligonucleotide during its manufacturing on solid support. However, attempts to condense **1** with either the squalene derivative **2** or its more electrophilic C-5 nitro analogue **3** met with repetitive failure (data not shown). We thus envisioned that the challenging squalenoylation might be more efficiently achieved by the use of the maleimide group as thiol acceptor as previously described by Weber et al.[27] Toward this goal, the maleimide squalene **4** was prepared from the corresponding aminosqualene by condensation with *N*-(ethoxycarbonyl)maleimide **6** (Scheme 1). However, attempts at coupling siRNA **1** with **4** in a PBS (phosphate buffered saline) solution/DMF mixture were similarly found fruitless, providing only a minute amount of the desired conjugate (5%) based on the HPLC trace and MALDI-TOF MS analysis.

In order to increase the maleimide functional group accessibility to the thiol-modified ON, we have intercalated a small ether linker between the maleimide group and the SQ moiety. The synthesis of the requisite squalenoyl maleimide **5** is outlined in

dx.doi.org/10.1021/jm2000272 |*J. Med. Chem.* 2011, 54, 4067–4076

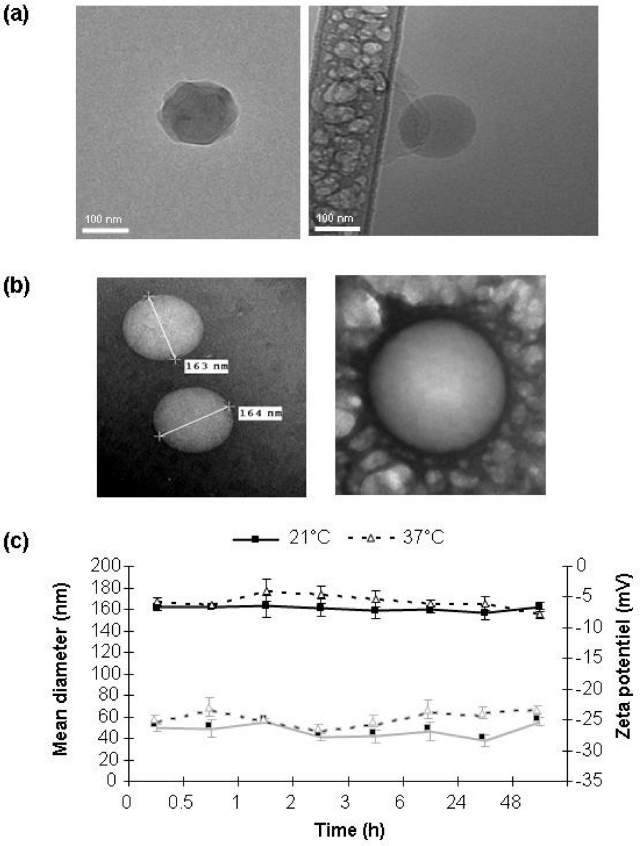

Figure 3. Characterization of RET/PTC1 siRNA-SQ NPs. Representative images of the RET/PTC1 siRNA-SQ NPs obtained by (a) cryoelectron microscopy and by (b) transmission electron microscopy. RET/PTC1 siRNA-SQ NPs were found to be spherical in shape. The nanoparticle size, as observed by TEM, correlated well with the size measured by laser light scattering (Nanosizer). (c) Mean diameter (black curves) and ζ potential (gray curves) evolution of RET/PTC1 siRNA-SQ NPs upon incubation in water at room temperature and at 37 °C. Both size and ζ potential of RET/PTC1 siRNA-SQ NPs remained nearly constant after incubation for 48 h at room temperature and at 37 °C (n = 3 experiments).

the Scheme 1. Briefly, the maleimide moiety was first tethered with an ethoxyethanol linker according to the method of Keller and Rudinger[28] starting from *N*-(ethoxycarbonyl)maleimide **6**. Condensation of the resulting maleimide alcohol **7** with the mixed anhydride derived from 1,1′,2-tris-norsqualenic acid **8**[23] and ethyl chloroformate provided adduct **5** in 35% yield. (Scheme 1). Nevertheless, we observed no significant increase in the reaction yield (7%) with the siRNA (Figure 2a, chromatogram 1), although fewer byproducts were formed than with maleimide **4**. By contrast, when 50% of methanol was added as cosolvent, the adduct **9** was obtained in 45% yield. A further improvement was gained when microwave irradiation (10 min, 70 °C) was substituted to the conventional heating, providing the desired squalenoyl oligonucleotide **9** in 55% yield (Figure 2a, chromatogram 2). Calculated RET/PTC1 siRNA conjugate weight was 7365 Da, in agreement with the MALDI-TOF mass spectrometry determined weight 7365.14 Da (Figure 2b). Purification of the crude product on polymeric RP-HPLC column and lyophilization then afforded the pure squalenoyl-modified oligonucleotide **9** which was characterized by MALDI mass

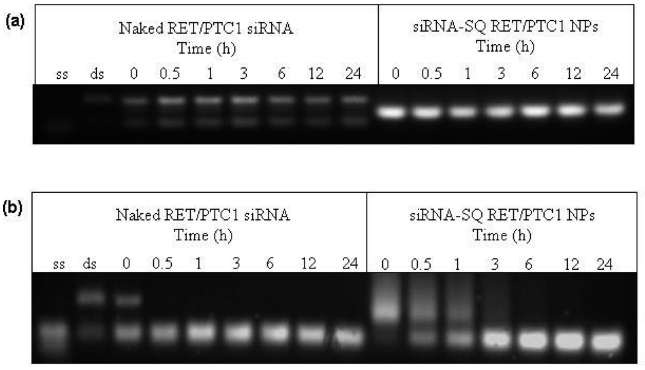

Figure 4. Serum stability of naked siRNA compared with RET/PTC1 siRNA-SQ NPs. NPs were incubated in (a) serum free media or (b) 10% serum containing media at 37 °C from 0 to 24 h. (a) In serum-free media, a total dissociation of the siRNA duplex from the first second was observed for naked siRNA (a, left panel). RET/PTC1 siRNA-SQ NPs were stable for 24 h (a, right panel). (b) In serum-containing media, the RET/PTC1 siRNA-SQ NP increased the stability of the siRNA duplex from 0 to 1 h postincubation (compare left to right panel).

spectrometry. Although we may expect that the conjugate addition of the thiol group on the maleimide double bond gave a mixture of two diastereomers, only one peak was observed in the HPLC trace. Given the sizes of both the oligonucleotide and the squalene with respect to the maleimide ring and the conformational flexibility around the linker, we hypothesize that this supplementary asymmetric center will be without repercussion.

The modification of the siRNA thiol backbone with squalenic acid at the 3′-end of the sense strand was found to dramatically enhance the lipophilicity as represented by the delayed elution times (Table 1).

RESULTS AND DISCUSSION

RET/PTC1 siRNA-SQ Nanoparticles Characterization. Purified RET/PTC1 siRNA-SQ sense strand **9** and RET/PTC1 siRNA antisense strand were hybridized, and duplex formation was assessed by 4% agarose gel electrophoresis (data not shown). The attachment of a squalene moiety with the siRNA duplex induced the spontaneous formation of siRNA-SQ nanoparticles in H_2O (control siRNA-SQ and RET/PTC1 siRNA-SQ NPs) with a size of 165 ± 10 nm and a polydispersity index of 0.2 as measured by laser light scattering (number of measurements n = 10). This emphasizes the important contribution of the squalene to the overall physicochemical behavior of the conjugate, as also illustrated by the impressive increase in the lipophilic character of RET/PTC1 siRNA-SQ shown by RP-HPLC analysis. RET/PTC1 siRNA-SQ NPs dimension was confirmed by electronic microscopy and cryotransmission electron microscopy showing spherical regular particles without visible supramolecular organization, as illustrated in Figure 3a and Figure 3b. The nanoparticles were found to be negatively charged, with a mean ζ potential of −26 mV, which is in favor of the establishment of repulsive forces allowing the stabilization of the NPs suspension; both size and ζ potential of RET/PTC1 siRNA-SQ NPs remained nearly constant after incubation for 48 h at room temperature and at 37 °C (Figure 3c). Then the stability of the RET/PTC1 siRNA-SQ duplex in nanoparticle formulation was tested in vitro for 24 h in 10% serum-containing media and in serum free media, relative to the naked RET/PTC1 siRNA. In both conditions, the stability of RET/PTC1

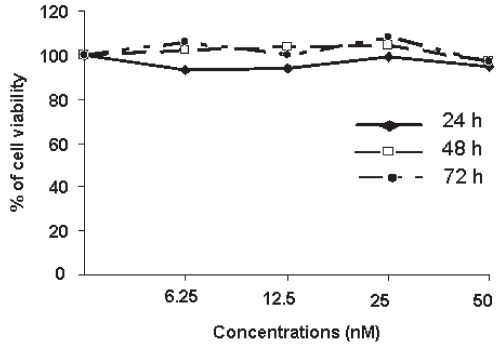

Figure 5. Cell viability at different concentrations of RET/PTC1 siRNA-SQ NPs. MTT assay was performed on BHP 10-3 cells as described in Experimental Section. Cell viability was calculated as $100 \times [(\text{A570 of NP treated cells} - \text{A570 of blank})]/[(\text{A570 of control cells} - \text{A570 of blank})]$. No statistical difference was observed between untreated cells and RET/PTC1 siRNA-SQ NP treated cells at 24, 48, and 72 h.

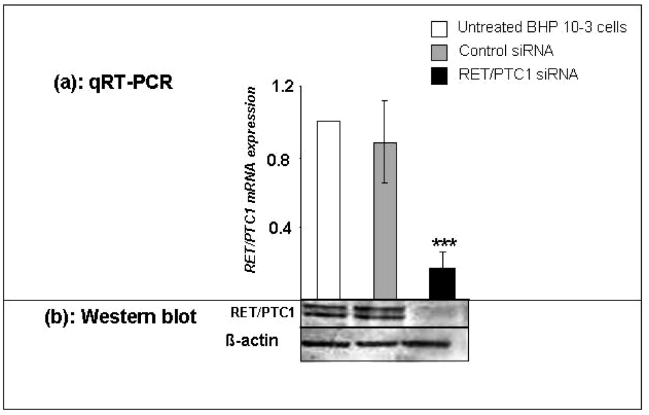

Figure 6. Gene silencing efficiency of RET/PTC1 siRNA in the BHP 10−3 cell line. (a) The *RET/PTC1* mRNA expression was analyzed by real time quantitative reverse transcription PCR (qRT-PCR) for treated cells by siRNA RET/PTC1 (black) or siRNA CT (gray) and compared to untreated cells (white). Experiments were performed 24 h after transfection with 50 nM RET/PTC1 siRNA or control siRNA using Lipofectamine 2000. Measurement shows a reduction of RET/PTC1 mRNA levels after transfection of RET/PTC1 siRNA. The bars represent the mean ± SD of three independent experiments: (***) Significant change compared to untreated cells using ANOVA followed by Bonferroni's test ($p < 0.001$). (b) RET/PTC1 protein level in untransfected and transfected cells with RET/PTC1 siRNA or CT siRNA at 50 nM. Proteins were extracted 24 h after transfection and analyzed by Western blot using Ret antibody. β-Actin was used as loading control for Western blot. Experiments were performed in triplicate.

siRNA-SQ NPs was improved relative to the naked RET/PTC1 siRNA in solution. In serum free media, naked siRNA displayed immediate and complete dissociation of the duplex (Figure 4a, left panel), whereas RET/PTC1 siRNA-SQ NPs were stable until 24 h (Figure 4a, right panel). In serum-containing media, the RET/PTC1 siRNA-SQ NP also increased the stability of the siRNA duplex from 0 to 1 h postincubation (Figure 4b, compare left to right panel). Thus, nanoparticles have clearly improved the nucleic acid stability in both serum and serum free media. This should allow an improved cell/tissue delivery of RET/PTC1, since its stability during 1 h in serum conditions may be sufficient to reach the tumor as an intact molecule.

In Vitro Evaluation. MTT assay did not show any significant inhibition of growth rate for RET/PTC1 siRNA-SQ NPs treated cells when compared to untreated cells after 24, 48, and 72 h incubations. This experiment was done for TPC-1 cells (data not shown) and for BHP 10-3 cells (Figure 5). It was observed that ~95% of the cells were still metabolically active after RET/PTC1 siRNA-SQ NPs treatment. By qRT-PCR we found that the RET/PTC1 siRNA significantly reduced *RET/PTC1* mRNA levels by ~80%, whereas the control siRNA did not show any statistical difference when compared with untreated cells (Figure 6a). The down-regulation of *RET/PTC1* mRNA levels by siRNA was paralleled by a decrease in RET/PTC1 protein content (Figure 6b). Thus, the cytotoxicity of RET/PTC1 siRNA-SQ NPs was evaluated in this model, but no cell growth inhibition was noted and the absence of *RET/PTC1* gene silencing was observed too (data not shown), possibly because in cell culture conditions, the limited enzymatic content did not allow the cleavage of the squalene needed for nanoparticle disaggregation before further mRNA sequence recognition. From the other side, this experiment has also highlighted the absence of any cell toxicity using squalene nanoparticles as noncationic nanocarriers of siRNA.

In Vivo Evaluation. In a preliminary experiment, we have tested the tumorigenicity of the TPC-1 and BHP 10-3 cells in nude mice. It was observed that TPC-1 cells were not able to form tumors, whereas BHP 10-3 were tumorgenic after subcutaneous injection of 10^6, 2.5×10^6, and 5×10^6 cells. Then the efficiency of RET/PTC1 siRNA-SQ NPs was tested on BHP 10-3, 2.5×10^6 cells subcutaneously inoculated into irradiated nude mice. When tumors reached around 50 mm^3, mice were treated by 2.5 mg/kg in five intravenous injections as described in Experimental Section. The ANOVA test followed by Bonferroni's test showed a statistical difference between treatments ($p = 0.01$). RET/PTC1 siRNA-SQ NP significantly reduced the tumor size with a tumor growth inhibition rate of 70% ($p < 0.05$), whereas the control siRNA-SQ NP did not significantly inhibit the tumor growth ($p > 0.05$) compared to the control saline (Figure 7a). Then the silencing ability of RET/PTC1 siRNA-SQ NPs was assessed in three tumor biopsies by qRT-PCR and the protein content by Western blot. By qRT-PCR it was found that RET/PTC1 siRNA-SQ NPs significantly reduced *RET/PTC1* mRNA levels by approximately 80%, whereas the control siRNA-SQ NPs did not show any statistical difference when compared to the control saline (Figure 7b). The down-regulation of *RET/PTC1* mRNA levels by RET/PTC1 siRNA-SQ NPs was paralleled by a decrease in RET/PTC1 protein content (Figure 7c).

Thus, whereas RET/PTC1 siRNA-SQ NPs did not display any cytotoxicity in vitro, significant regression of tumor growth (i.e., 70%) was observed in vivo with the RET/PTC1 siRNA-SQ NPs, whereas the control siRNA-SQ NPs injected under the same conditions failed to do so. This in vivo anticancer activity was even paralleled by RET/PTC1 oncogene and oncoprotein expressions inhibition, revealing that at least a fraction of the intravenously injected siRNA was delivered in an active form inside the tumor cells. These data demonstrate once again that prediction of in vivo pharmacological efficacy through cell culture experiments is uncertain, even when experiments are performed on exactly the same tumor cell line. We have already observed such a phenomenon with siRNA loaded onto chitosan-coated nanospheres.[26] The reasons are numerous: (i) Cells in culture may exhibit different pattern of gene expression and

dx.doi.org/10.1021/jm2000272 |J. Med. Chem. 2011, 54, 4067–4076

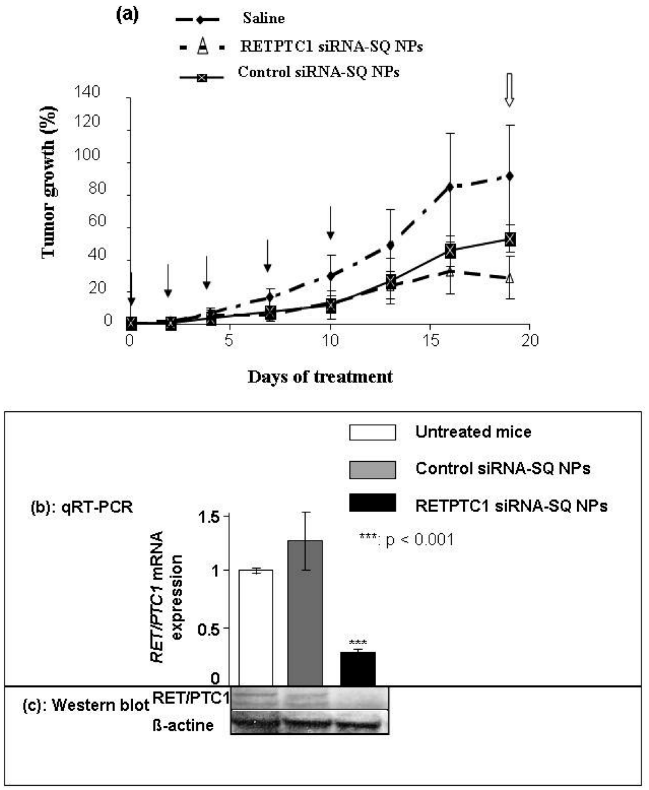

Figure 7. Antitumor effects of the RET/PTC1 siRNA-SQ NPs. (a) The treatment was performed by intravenous administration until day 10. Arrows correspond to the days of treatment. Five injections were performed for [RET/PTC1 or control] siRNA-SQ NPs at days 0, 2, 4, 7, and 10 at 2.5 mg/kg cumulative dose. Downward arrows indicate that mice were sacrificed at day 19. The effects of RET/PTC1 siRNA-SQ NPs on tumor growth in nude mice are expressed relative to tumor volume on day 1 according to the following formula: (tumor volume at day x)/(tumor volume at day 1). Bars correspond to the standard deviation for five mice. A statistical difference was observed between treatments ($p = 0.01$) using the ANOVA test followed by Bonferroni test who showed a statistical difference between RET/PTC1 siRNA-SQ NPs and untreated mice (saline), $p = 0.013$. (b) qRT-PCR shows that the RET/PTC1 siRNA-SQ NPs inhibit RET/PTC1 expression into mice grafted tumors and that the control siRNA-SQ NPs have no effect on RET/PTC1 expression compared to untreated mice ($n = 3$ tumors): (***) $p < 0.001$. (c) By Western blot we found a decrease in RET/PTC1 protein expression (three independent experiments).

differentiation than in vivo. (ii) The physicochemical properties of the nanoparticles may change in vivo: aggregation, dissociation, or reorganization due to physiological salts, opsonins, lipids, etc. (iii) The cell culture experiments that are performed usually during 24 h are far from in vivo experiments that lasted weeks, and (iv) the enzymatic content is entirely different in vitro than in vivo. This should significantly influence the kinetic release of the oligonucleotide from the squalenoylated nanoparticles.

CONCLUSION

The linkage of RET/PTC1 siRNA to squalene at the 3′-terminus of the sense strand via maleimide−sulfhydryl chemistry led to amphiphilic molecule that self-organized in water as nanoparticles. In vitro, this bioconjugate did not show any cytotoxicity in two human PTC cells. Interestingly, in vivo, on a mice xenografted RET/PTC1 experimental model, RET/PTC1 siRNA-SQ NPs were found to inhibit tumor growth and RET/PTC1 oncogene and oncoprotein expression after 2.5 mg/kg cumulative dose intravenous injections. Thus, using RET/PTC1 siRNA as a model, we propose here an original noncationic nanoplate-form for the efficient delivery of small fragments of nucleic acids and open the way to further pharmacological studies.

EXPERIMENTAL SECTION

General. IR spectra were obtained as solid or neat liquid on a Fourier transform Bruker Vector 22 spectrometer. Only significant absorptions are listed. The ^{1}H and ^{13}C NMR spectra were recorded on Bruker Avance 300 (300 and 75 MHz for ^{1}H and ^{13}C, respectively). Recognition of methyl, methylene, methine, and quaternary carbon nuclei in ^{13}C NMR spectra rests on the J-modulated spin−echo sequence. Mass spectra were recorded on a Bruker Esquire-LC. Analytical thin-layer chromatography was performed on Merck silica gel 60F_{254} glass precoated plates (0.25 mm layer). Column chromatography was performed on Merck silica gel 60 (230−400 mesh ASTM). All the chemicals used were of analytical grade. Water was purified using a Milli-Q system (Millipore, St.-Quentin-en-Yvelines, France). Tetrahydrofuran (THF) was distilled from sodium/benzophenone ketyl. Methanol and ethanol were dried over magnesium and distilled. DMF and CH_2Cl_2 were distilled from calcium hydride, under a nitrogen atmosphere. All reactions involving air- or water-sensitive compounds were routinely conducted in glassware that was flame-dried under a positive pressure of nitrogen. Squalene, ethyl chloroformate, and 2-(2-aminoethoxy)ethanol were purchased from Sigma-Aldrich Chemical Co., France. Chemicals obtained from commercial suppliers were used without further purification. HPLC grade acetonitrile, methanol, ethanol, and acetone were provided by Carlo Erba (Rodano, Italy). Triethylammonium acetate (TEAA) buffer was obtained from Fluka BioChemika. Helium for mobile phase degassing was from Air Liquide. After HPLC purification, the final siRNA−squalene bioconjugate compound was further subjected to liquid chromatography. The purity was calculated from the LC chromatogram at a wavelength of 258 nm. By this method, the purity was greater than or equal to 95.0%.

1-(4,8,13,17,21-Pentamethyldocosa-4,8,12,16,20-pentaenyl)pyrrole-2,5-dione (4). To a well-stirred suspension of 1,1′,2-trisnor-aminosqualene (250 mg, 0.64 mmol) in saturated sodium bicarbonate aqueous solution (3 mL) was added dropwise a solution of *N*-(ethoxycarbonyl)maleimide (**6**) (110 mg, 0.65 mmol) in CH_2Cl_2 (2 mL). The reaction mixture was stirred at 20 °C for 1 h. CH_2Cl_2 (10 mL) was added, and the organic layer was separated. The aqueous phase was extracted with CH_2Cl_2 (2 × 5 mL). The combined organic phases were washed with brine, dried over $MgSO_4$, and concentrated under reduced pressure to provide a yellow oil. The residue was taken into anhydrous ethanol (10 mL), and DABCO (15 mg, 0.13 mmol) was added. The reaction mixture was heated at reflux for 2 h. After cooling, the solution was concentrated under reduced pressure, taken into AcOEt (15 mL), and sequentially washed with 0.5 M HCl and brine. The organic phase was dried over $MgSO_4$ and concentrated under reduced pressure. Chromatographic purification on silica gel, eluting with AcOEt/cyclohexane 1:1, afforded maleimido squalene **4** as a colorless oil (150 mg, 48%). IR (neat) ν: 2913, 2845, 1710, 1695, 1442, 1408, 1374, 1333, 1142, 1110, 841, 826. ^{1}H NMR ($CDCl_3$, 300 MHz): δ = 6.67 (s, 2H, OCC*H*=C*H*CO), 5.18−5.03 (m, 5H, *H*C=C(CH_3)), 3.47 (t, J = 7.4 Hz, 2H, CH_2CH_2N), 2.10 −1.90 (m, 20H), 1.67 (s, 3H, (CH_3)$_2$C=), 1.60 (s, 15H). ^{13}C NMR ($CDCl_3$, 75 MHz): δ = 170.8 (2C, OCCH=CHCO), 135.1 (C, HC=*C*(CH_3)), 135.0 (C, HC=*C*-(CH_3)), 134.9 (C, HC=*C*(CH_3)), 134.0 (2CH, OCCH=CHCO), 133.4 (C, HC=*C*(CH_3)), 131.2 (C, HC=*C*(CH_3)), 125.1 (CH, HC=C(CH_3)), 124.4 (CH, HC=C(CH_3)), 124.3 (3CH, *H*C=C-(CH_3)), 39.7 (2CH_2), 39.6 (CH_2), 37.7 (CH_2), 36.7 (CH_2), 28.2

dx.doi.org/10.1021/jm2000272 |J. Med. Chem. 2011, 54, 4067–4076

($2CH_2$), 26.8 (CH_2), 26.6 ($2CH_2$), 26.5 (CH_2), 25.6 (CH_3, $(CH_3)_2C$=), 17.6 (CH_3), 16.0 ($3CH_3$), 15.7 (CH_3). HRMS (+ESI): m/z 466.3686 ($[M + H]^+$ calcd for $C_{31}H_{48}NO_2$ 466.3685).

2-[2-(2,5-Dioxo-2,5-dihydro-1*H*-pyrrol-1-yl)ethoxy]ethyl (4*E*,8*E*,12*E*,16*E*)-4,8,13,17,21-Pentamethyl-docosa-4,8,12,16,20-pentaenoate (5). To an ice-cooled solution of squalenic acid 8 (400 mg, 1.0 mmol) in THF (4 mL) was added triethylamine (121 mg, 1.2 mmol) followed by ethyl chloroformate (114 mg, 1.05 mmol). The resulting mixture was stirred at 0 °C for 30 min. A solution of alcohol **7** (203 mg, 1.1 mmol) in THF (2 mL) was added dropwise, and the mixture was stirred at 20 °C for 24 h. The mixture was concentrated under reduced pressure, and the residue was treated with 1 M HCl (2 mL). The mixture was extracted with CH_2Cl_2 (3 × 20 mL). The combined organic layers were washed with brine, dried over $MgSO_4$, and concentrated under reduced pressure to provide a reddish oil. Chromatographic purification on silica gel, eluting with pentane/ether 3:1, gave 198 mg (35% yield) of maleimide **5** as a colorless oil. IR (neat) ν: 3000−2800, 1737, 1710, 1438, 1406, 1386, 1321, 1295, 1135, 1110, 1043, 976, 828. ^{1}H NMR ($CDCl_3$, 300 MHz): δ = 6.70 (s, 2H, OCC*H*=C*H*CO), 5.15−5.02 (m, 5H, *H*C=C(CH_3)), 4.16 (t, J = 4.5 Hz, 2H,) 3.74−3.71 (m, 2H), 3.70−3.60 (t, J = 4.8 Hz, 4H), 2.40−2.35 (m, 2H), 2.30−2.20 (m, 2H), 2.10−1.90 (m, 16H), 1.66 (s, 3H, $(CH_3)_2$C=), 1.60 (s, 15H). ^{13}C NMR (acetone-d_6, 75 MHz): δ = 172.8 (2C, OCCH=CHCO), 171.1 (C, CO_2), 135.2 (C, HC=*C*-(CH_3)), 135.1 (C, HC=*C*(CH_3)), 135.0 (C, HC=*C*(CH_3)), 134.8 (2CH, OCCH=*C*HCO), 133.9 (C, HC=*C*(CH_3)), 131.2 (C, HC=*C*-(CH_3)), 125.3 (CH, HC=C(CH_3)), 124.8 (3CH, *H*C=C(CH_3)), 124.7 (CH, *H*C=C(CH_3)), 68.7 (CH_2), 67.7 (CH_2), 63.4 (CH_2), 40.1 ($2CH_2$), 39.9 (CH_2), 37.3 (CH_2), 35.0 (CH_2), 33.2 (CH_2), 28.5 ($2CH_2$), 27.1 (CH_2), 26.9 (CH_2), 26.8 (CH_2), 25.5 (CH_3, $(CH_3)_2$C=), 17.4 (CH_3), 15.8 ($2CH_3$), 15.7(CH_3), 15.6 (CH_3). MS (+ESI): m/z (%) = 590.6 (100) $[M + Na]^+$. HRMS (+ESI): m/z 590.3826 ($[M + Na]^+$ calcd for $C_{35}H_{53}NO_5Na$ 590.3826).

siRNAs Used and Chemical Modifications. The RET/PTC1 siRNA and the irrelevant siRNA scrambled sequence used as a control in the experiments were previously described.[9] The siRNA sequences were as follows: RET/PTC1 siRNA sense strand, 5′-r(CGU UAC CAU CGA GGA UCC A)d(AA)-3′; RET/PTC1 siRNA antisense strand, 5′-r(U GGA UCC UCG AUG GUA ACG)d(CT)-3′; control siRNA sense strand, 5′-r(GCCAGUGUCACCGUCAAGG)d(AG)-3′; control siRNA antisense strand, 5′-r(CCU UGA CGG UGA CAC UGG C) d(TT)-3′.

All single-stranded RNAs were synthesized by Eurogentec (Belgium) and were characterized by matrix assisted laser desorption/ionization time-of-flight mass spectrometry (MALDI-TOF MS) and purified by RP-HPLC. Single-stranded RNAs were synthesized as 19-mers with two -3′ overhanging 2′-deoxynucleotides residues to provide stabilization against nucleases as described by Tuschl et al.[27] To allow functionalization, a 3-mercaptopropyl phosphate group was introduced at the 3′-end of the sense strand of each siRNA sequence (**1**, Figure 1).

To generate siRNA from RNA single strands, equimolar amounts of both forward and reverse strands were annealed in annealing buffer [30 mM HEPES-KOH (pH 7.4), 2 mM Mg acetate, 100 mM K acetate] for 1 min at 95 °C and then kept 1 h at room temperature before storing at −20 °C.

Synthesis and Characterization of RET/PTC1 siRNA−Squalene Bioconjugate. Thiol modified RET/PTC1 siRNA sense strand **1** (0.33 mg, 0.05 nmoles) in 667 μL of PBS (0.1 M, pH 7) was mixed with squalenoyl maleimide 5 (3.33 mg, 5.86 nmoles) in 33 μL of DMF and 30% methanol with a molecular ratio of RNA/SQ (1:100). The reaction mixture was activated in microwave (10 min, 70 °C) under magnetic stirring. The solution was lyophilized, and the residue was washed with ethanol and acetone (3 × 1 mL) to eliminate the excess squalenoyl maleimide, air-dried, and then dissolved in 1 mL of RNase free water. The progress of the reaction and purification was monitored by RP-HPLC on a polymeric column as described below. The coupling yield was determined based on the UV absorbance of the species. The identity of the conjugate was confirmed by MALDI-TOF mass spectrometry.

HPLC Equipment and Conditions. The HPLC separation was performed on a Waters high-performance liquid chromatography system equipped with a photodiode array detector (Waters 2996) whose wavelength range was between 190 and 800 nm, a pump (model Waters 600 controller), and an automatic injector (Waters 717 autosampler). The stationary phase consists of a nonporous, alkylated poly(styrene divinylbenzene) column (Hamilton 10 μm, 4.6 mm × 250 mm, PEEK) protected by precolumn (Hamilton). The data acquisition software is Empower. Flow rate was 1.2 mL/min. Injection volumes were 100 μL. The column temperature was maintained at 20 °C throughout the separation. Chromatography was performed using two mobile phases A and B. Mobile phase A consisted of an aqueous solution of 0.2 M TEAA (5%), pH 7.0, with 5% acetonitrile (v/v), and mobile phase B consisted of 95% acetonitrile with 5% TEAA (v/v). All solvents were degassed ultrasonically. Chromatograms were recorded at a wavelength of 258 nm. Quantification of peaks was performed by integration of peak areas. RP HPLC analyses were performed using the following gradient condition: 0−8 min linear gradient from 0% to 24% of B; 8−16 min linear gradient from 24% to 90% of B; 16−18 min back to 0% B; and 18−28 min re-equilibration with 100% of A. siRNA for downstream uses were purified by manual peak collection. Fractions were collected for 1 min, corresponding to a fraction volume of 1.2 mL, and then were lyophilized. All lyophilized siRNA fractions were reconstituted in DEPC-treated water.

MALDI-TOF Mass Spectrometry. Matrix-assisted laser desorption ionization (MALDI) tandem mass spectrometry was performed with a Perseptive Voyager DE STR MALDI time-of-flight (TOF) mass spectrometer (Perseptive Biosystems) equipped with a Tektronix TDS 540C digital oscilloscope (500 MHz, digitization rate 2 gigasample·s^{-1}) and with a N_2 laser at the IMAGIF/ICSN, Gif-sur-Yvette, France.

Cells and Cell Culture. Two human papillary thyroid carcinoma cell lines, TPC-1, kindly provided by Dr. C. Dupuy (UMR 8200 CNRS, IGR, Villejuif, France), and BHP 10-3,[28] kindly provided by Dr. Clayman Gary (MD Anderson Cancer Center, Houston), harboring the RET/PTC1 rearrangement were used. Cells were maintained at 37 °C, 5% CO_2 in Dulbecco's modified Eagle medium (DMEM) (Invitrogen, France). Medium was supplemented with 10% fetal calf serum (FCS), 100 U/mL penicillin, and 100 mg/mL streptomycin (Invitrogen, France). The volume of cell culture medium used during experiments was 2 mL/well for cells cultured in six-well plates.

Transfection Experiments. Transfections of RET/PTC1 siRNA or of control siRNA were carried out using Lipofectamine 2000 transfection reagent (Invitrogen, France) on TPC-1 and BHP 10-3 cells according to the manufacturer's instructions. Transfections were performed in serum-free OPTI-MEM using a siRNA concentration of 50 nM and 6 μL of Lipofectamine 2000 as described by Gilbert-Sirieix et al.[9]

RNA Extraction and Real Time Quantitative Reverse Transcription PCR (qRT-PCR) Analysis. For the determination of the RET/PTC1 expression, total RNAs of untreated cells, RET/PTC1 siRNA, and control siRNA transfected cells were extracted using RNeasy mini-kit (Qiagen Ltd., West Sussex, U.K.). Total RNA quantity and quality were assessed using the Nanodrop ND-1000 spectrophotometer (Wilmington, U.S.). M-MLV reverse transcriptase buffer pack (Promega, France) was used for reverse transcription. Briefly, 1 μg of total RNA was incubated in a 20 μL final volume of M-MLV RT for 1 h at 42 °C. Then RET/PTC1 mRNA expression was determined by qRT-PCR on 1 μL of the reverse transcription product in a 25 μL final volume. The following primers were used for RET/PTC1 amplification (290 bp): forward 5′-AGATAGAGCTGGAGACCTAC-3′ and reverse

5′-CTGCTTCAGGACGTTGAA-3′. RPL 13A forward 5′-AGATAGAGCTGGAGACCTAC-3′ and reverse 5′-CTGCTTCAGGACGTTGAA-3′ primers were used as an internal gene control. The amplification was monitored on ABI PRISM 7000 Taqman (Applied Biosystems, Perkin-Elmer) using SYBR GreenER qPCR Supermix for ABI PRISM (Invitrogen, France) according to the manufacturer's instructions. Samples were run in duplicate with primer sets of the gene of interest and the RPL 13A control gene. Gene regulation was determined by the $2^{-\Delta\Delta Ct}$ method[29,30] and normalized to RPL13A levels for human cell lines.[31] The results are given as relative fold compared with untreated cells.

Protein Extraction and Western Blot Analysis. For Western blot analysis, total protein extracts were obtained using M-PER reagent (Thermo Scientific, Pierce) with protease inhibitors cocktail (Roche). Proteins were titrated by the BCA method using the BCA protein assay (Thermo Scientific, Pierce). An amount of 30 μg of cell extracts was boiled in Laemmli loading buffer and separated on 10% sodium dodecyl sulfate−polyacrylamide electrophoresis gel. Proteins were transferred using the iBlot dry blotting system (Invitrogen, France) on precut nitrocellulose membranes and then blocked with 0.2% casein (I-Block reagent, Tropix) in PBS with 0.1% Tween-20. The membranes were incubated overnight at 4 °C with the primary antibodies specific for RET (C-19: sc-167; Abgene 1:200) or β-actin (rabbit polyclonal, 1:1000; Sigma-Aldrich Chimie S.a.r.l.) used as an internal control. Blots were washed and incubated with anti-rabbit antibody conjugated to alkaline phosphatase (1:20,000, Tropix) for 1 h at room temperature and subsequently washed and revealed using CDP Star chemoluminescence reagent (Perkin-Elmer).

Preparation and Characterization of RET/PTC1 siRNA-SQ Nanoparticles. RET/PTC1 siRNA-SQ NPs were prepared by nanoprecipitation as follows. Purified squalene modified RET/PTC1 siRNA sense strand and RET/PTC1 siRNA antisense strand were hybridized, and duplex formation was assessed by 4% agarose gel electrophoresis. Then 20 μM RET/PTC1 siRNA-SQ bioconjugate was first lyophilized and then dissolved in 0.5 mL of ethanol and added dropwise under magnetic stirring (500 rpm) into 1 mL of a 5% aqueous dextrose solution. Then ethanol was completely evaporated using a Rotavapor to obtain an aqueous suspension of pure RET/PTC1 siRNA-SQ nanoassemblies. Control siRNA-SQ NPs were prepared using the same protocol as described above.

Particle Size Measurement. The hydrodynamic diameter of the nanoparticles was measured at 20 °C by quasi-elastic light scattering using a Nanosizer 4 (Malvern Instrument Ltd., France), operating at 90 °C. Practically, an amount of 100 μL of the suspension was diluted in 0.9 mL of Milli-Q water. The temperature was allowed to equilibrate 5 min before measurement. The results gave the mean hydrodynamic diameter of the dispersed particles obtained from three independent determinations. The standard deviation of the size distribution and the polydispersity index were also given.

ζ Potential Determination. The ζ potential of the RET/PTC1 siRNA-SQ NP was determined as follows. Dilution of the nanoparticles suspension [1:10 (v/v)] was performed in 1 mM NaCl and analyzed with a Zetasizer 4 (Malvern Instrument Ltd., France).

In order to assess the stability of the nanoparticles suspension, 0.2 μM RET/PTC1 siRNA-SQ NPs were incubated at room temperature and at 37 °C for 0.5, 1, 2, 3, 6, 24, and 48 h. Size and ζ potential were measured at different time points.

Transmission Electron Microscopy and Cryotransmission Electron Microscopy. Transmission electron microscopy (TEM) was performed using a Philips EM208 with a large format CCD camera AMT at the CCME Orsay. The samples were deposited on a carbon-coated form war film on copper grids. After 5 min, the excess was removed and stained with neutral 1% aqueous phosphotungstic acid during 30 s. For cryoelectron microscopy, samples were pipetted on to holey grids in a humid chamber, blotted with filter paper for 15 s, and quick-frozen by plunging them in liquid ethane cooled with liquid N_2. Images were taken at 200 kVat a magnification of 3000×.

Stability of RET/PTC1 siRNA-SQ NPs in Serum and in Serum-Free Medium. Serum stability of an aqueous solution of naked RET/PTC1 siRNA vs RET/PTC1 siRNA-SQ NP was assessed using a 4% agarose gel electrophoresis stained with ethidium bromide. Then 5 μM naked RET/PTC1 siRNA and RET/PTC1 siRNA-SQ NPs were incubated in serum free medium and in medium containing 10% fetal calf serum at 37 °C. At each predetermined time point (0, 0.5, 1, 3, 6, 12, and 24 h), aliquots of each sample (10 μL) were collected and stored at −20 °C. Then 1 μL of 100 bp DNA ladder (Interchim, Montluçon, France) was run alongside the products.

Cytotoxicity Assay. Cytotoxicity of nanoparticles was evaluated on BHP 10-3 cells by the MTT (3-(4,5-dimethylthiazol-2-yl)-2,5-diphenyltetrazolium bromide) method.[32] The cells were seeded in 12-well plates (1.5×10^5 cells per well) and incubated with 1 mL of Dulbecco's modified eagle medium (DMEM) containing 10% fetal calf serum and antibiotics (100 U/mL penicillin, 100 μg/mL streptomycin) at 37 °C, 5% CO_2. After 24 h, the cell culture medium was replaced by 1 mL of fresh culture medium and treated with RET/PTC1 siRNA-SQ NP at different concentrations (i.e., 6.25, 12.5, 25, and 50 nM). After 24, 48, and 72 h postincubation at 37 °C, 100 μL of MTT reagent (5 mg/mL in PBS) (Sigma-Aldrich, Saint Quentin Fallavier, France) were added in each well. After 2 h of incubation at 37 °C, the cells were lysed by 1 mL of a 10% sodium dodecyl sulfate (SDS) in 10 mM HCl solution overnight at 37 °C. An amount of 200 μL of the medium contained in each well was then transferred to a 96-well plate, and the optical density was measured at 570 nm wavelength using a microplate reader (MRXII photometer, Dynex Technology). Untreated cells were used as a control. Each nanoparticle concentration condition was tested twice, and each measurement was made in duplicate. Results are expressed as a percentage of untreated cells.

siRNA Administration to Nude Mice. All animal experiments were carried out according to the French laws of animal welfare and were approved by the Ethics Commission of the official veterinary authorities. First, we performed tumorigenicity tests of TPC-1 and BHP 10-3 cells on nude mice produced by the laboratory. One day before tumor implantation mice were preirradiated by 5 Gy, then subcutaneous PTC tumors were induced by inoculation of 2.5×10^6 human BHP 10-3 cells in the right flank. When the tumor volume reached 40−50 mm^3, 3 groups of 5 mice were intravenously treated with either saline or with a cumulative dose of 2.5 mg/kg (RET/PTC1 or control) siRNA-SQ NPs dispersed in a 9 g/L NaCl solution given in 5 intravenous injections of 100 μL each at day 0, 2, 4, 7, and 10. After the first injection, the size and the volume of the tumors were evaluated over 19 days. Tumour size was measured in two dimensions with a calliper-like instrument. Individual tumor volumes (V) were calculated by the formula V = (length × [width]^2)/2. At the end of the experiment, the animals were sacrificed and tumors were excised and snap frozen immediately thereafter for qRT-PCR analysis and Western blotting.

RNA and Protein Extractions from Tumors. Three tumor biopsies of each group of animals were taken at the end of the experiments. Total RNA was extracted using RNeasy mini-kit (Qiagen Ltd., West Sussex, U.K.) according to the manufacturer's instructions. Then reverse transcription and qRT-PCR were performed as previously described.

The same tumors were used for total proteins extraction using M-PER reagent (Thermo Scientific, Pierce) with protease inhibitors cocktail (Roche) and analyzed by Western blot as described above.

Statistical Analysis. For in vitro and in vivo studies, data are presented as the mean ± SD. The mean values of treatment groups were compared with one-way ANOVA. When ANOVA showed that there were significant differences between the groups, Dunnett's test or Bonferroni's test was used to identify the sources of these differences. $p \leq 0.05$ was considered statistically significant.

■ ASSOCIATED CONTENT

Supporting Information. Reverse phase HPLC chromatogram of the purified RET/PTC1 siRNA-SQ and spectroscopic data for compounds **4** and **5**. This material is available free of charge via the Internet at http://pubs.acs.org.

■ AUTHOR INFORMATION

Corresponding Author

*For L.M.-M.: phone, 33 1 42 11 62 42; fax, 33 1 42 11 53 14; e-mail, liliane.massade@igr.fr. For P.C.: phone, 33 1 46 83 53 96; fax, 33 1 46 61 93 34; e-mail, patrick.couvreur@u-psud.fr.

■ ACKNOWLEDGMENT

The research leading to these results has received funding from the European Research Council under the European Community's Seventh Framework Programme FP7/2007-2013 Grant Agreement No. 249835.

■ ABBREVIATIONS USED

siRNA, small interfering RNA; PTC, papillary thyroid carcinoma; RET, rearranged during transfection; ON, oligonucleotide; RISC, RNA-induced silencing complex; TK, tyrosine kinase; RPL13A, ribosomal protein 13A; siRNA CT, siRNA control; qRT-PCR, real time quantitative reverse transcription PCR; Ct, cycle threshold; FCS, fetal calf serum; DMEM, Dulbecco's modified Eagle medium; SQ, squalene; NP, nanoparticle; TEAA, triethylammonium acetate; ddC, dideoxycytosine; MTT, 3-(4,5-dimethylthiazol-2-yl)-2,5-diphenyltetrazolium bromide; SDS, sodium dodecyl sulfate; THF, tetrahydrofuran; PBS, phosphate buffered saline; DMF, dimethylformamide; DABCO, 1,4-diazabicyclo[2.2.2]octane; DEPC, diethyl pyrocarbonate; RP-HPLC, reverse phase high-performance liquid chromatography; MALDI-TOF MS, matrix-assisted laser desorption ionization time-of-flight mass spectrometer; TEM, transmission electron microscopy

■ REFERENCES

(1) Gimm, O. Thyroid cancer. *Cancer Lett.* **2001**, *163*, 143–156.

(2) Hundahl, S. A.; Cady, B.; Cunningham, M. P.; Mazzaferri, E.; McKee, R. F.; Rosai, J.; Shah, J. P.; Fremgen, A. M.; Stewart, A. K.; Holzer, S. Initial results from a prospective cohort study of 5583 cases of thyroid carcinoma treated in the United States during 1996. U.S. and German Thyroid Cancer Study Group. An American College of Surgeons Commission on Cancer Patient Care Evaluation study. *Cancer* **2000**, *89*, 202–217.

(3) Smanik, P. A.; Furminger, T. L.; Mazzaferri, E. L.; Jhiang, S. M. Breakpoint characterization of the ret/PTC oncogene in human papillary thyroid carcinoma. *Hum. Mol. Genet.* **1995**, *4*, 2313–2318.

(4) Santoro, M.; Melillo, R. M.; Fusco, A. RET/PTC activation in papillary thyroid carcinoma: European Journal of Endocrinology Prize Lecture. *Eur. J. Endocrinol.* **2006**, *155*, 645–653.

(5) Santoro, M.; Melillo, R. M.; Carlomagno, F.; Fusco, A.; Vecchio, G. Molecular mechanisms of RET activation in human cancer. *Ann. N.Y. Acad. Sci.* **2002**, *963*, 116–121.

(6) DeLellis, R. A. Pathology and genetics of thyroid carcinoma. *J. Surg. Oncol.* **2006**, *94*, 662–669.

(7) Jhiang, S. M. The RET proto-oncogene in human cancers. *Oncogene* **2000**, *19*, 5590–5597.

(8) Mizuno, T.; Iwamoto, K. S.; Kyoizumi, S.; Nagamura, H.; Shinohara, T.; Koyama, K.; Seyama, T.; Hamatani, K. Preferential induction of RET/PTC1 rearrangement by X-ray irradiation. *Oncogene* **2000**, *19*, 438–443.

(9) Gilbert-Sirieix, M.; Ripoche, H.; Malvy, C.; Massaad-Massade, L. Effects of silencing RET/PTC1 junction oncogene in human papillary thyroid carcinoma cells. *Thyroid* **2010**, *20*, 1053–1065.

(10) Brummelkamp, T. R.; Bernards, R.; Agami, R. A system for stable expression of short interfering RNAs in mammalian cells. *Science* **2002**, *296*, 550–553.

(11) Bertling, W. M.; Gareis, M.; Paspaleeva, V.; Zimmer, A.; Kreuter, J.; Nurnberg, E.; Harrer, P. Use of liposomes, viral capsids, and nanoparticles as DNA carriers. *Biotechnol. Appl. Biochem.* **1991**, *13*, 390–405.

(12) Halder, J.; Kamat, A. A.; Landen, C. N., Jr.; Han, L. Y.; Lutgendorf, S. K.; Lin, Y. G.; Merritt, W. M.; Jennings, N. B.; Chavez-Reyes, A.; Coleman, R. L.; Gershenson, D. M.; Schmandt, R.; Cole, S. W.; Lopez-Berestein, G.; Sood, A. K. Focal adhesion kinase targeting using in vivo short interfering RNA delivery in neutral liposomes for ovarian carcinoma therapy. *Clin. Cancer Res.* **2006**, *12*, 4916–4924.

(13) Zimmermann, T. S.; Lee, A. C.; Akinc, A.; Bramlage, B.; Bumcrot, D.; Fedoruk, M. N.; Harborth, J.; Heyes, J. A.; Jeffs, L. B.; John, M.; Judge, A. D.; Lam, K.; McClintock, K.; Nechev, L. V.; Palmer, L. R.; Racie, T.; Rohl, I.; Seiffert, S.; Shanmugam, S.; Sood, V.; Soutschek, J.; Toudjarska, I.; Wheat, A. J.; Yaworski, E.; Zedalis, W.; Koteliansky, V.; Manoharan, M.; Vornlocher, H. P.; MacLachlan, I. RNAi-mediated gene silencing in non-human primates. *Nature* **2006**, *441*, 111–114.

(14) Soutschek, J.; Akinc, A.; Bramlage, B.; Charisse, K.; Constien, R.; Donoghue, M.; Elbashir, S.; Geick, A.; Hadwiger, P.; Harborth, J.; John, M.; Kesavan, V.; Lavine, G.; Pandey, R. K.; Racie, T.; Rajeev, K. G.; Rohl, I.; Toudjarska, I.; Wang, G.; Wuschko, S.; Bumcrot, D.; Koteliansky, V.; Limmer, S.; Manoharan, M.; Vornlocher, H. P. Therapeutic silencing of an endogenous gene by systemic administration of modified siRNAs. *Nature* **2004**, *432*, 173–178.

(15) Lv, H.; Zhang, S.; Wang, B.; Cui, S.; Yan, J. Toxicity of cationic lipids and cationic polymers in gene delivery. *J. Controlled Release* **2006**, *114*, 100–119.

(16) Kuo, W. T.; Huang, H. Y.; Huang, Y. Y. Intracellular trafficking, metabolism and toxicity of current gene carriers. *Curr. Drug Metab.* **2009**, *10*, 885–894.

(17) Thompson, M. P.; Chien, M. P.; Ku, T. H.; Rush, A. M.; Gianneschi, N. C. Smart lipids for programmable nanomaterials. *Nano Lett.* **2010**, *10*, 2690–2693.

(18) Wu, Y.; Sefah, K.; Liu, H.; Wang, R.; Tan, W. DNA aptamer-micelle as an efficient detection/delivery vehicle toward cancer cells. *Proc. Natl. Acad. Sci. U.S.A.* **2010**, *107*, 5–10.

(19) Wolfrum, C.; Shi, S.; Jayaprakash, K. N.; Jayaraman, M.; Wang, G.; Pandey, R. K.; Rajeev, K. G.; Nakayama, T.; Charrise, K.; Ndungo, E. M.; Zimmermann, T.; Koteliansky, V.; Manoharan, M.; Stoffel, M. Mechanisms and optimization of in vivo delivery of lipophilic siRNAs. *Nat. Biotechnol.* **2007**, *25*, 1149–1157.

(20) Godeau, G.; Staedel, C.; Barthelemy, P. Lipid-conjugated oligonucleotides via "click chemistry" efficiently inhibit hepatitis C virus translation. *J. Med. Chem.* **2008**, *51*, 4374–4376.

(21) Gissot, A.; Camplo, M.; Grinstaff, M. W.; Barthelemy, P. Nucleoside, nucleotide and oligonucleotide based amphiphiles: a successful marriage of nucleic acids with lipids. *Org. Biomol. Chem.* **2008**, *6*, 1324–1333.

(22) Miettinen, T. A.; Vanhanen, H. Serum concentration and metabolism of cholesterol during rapeseed oil and squalene feeding. *Am. J. Clin. Nutr.* **1994**, *59*, 356–363.

(23) Reddy, L. H.; Couvreur, P. Squalene: a natural triterpene for use in disease management and therapy. *Adv. Drug Delivery Rev.* **2009**, *61*, 1412–1426.

(24) Reddy, L. H.; Dubernet, C.; Mouelhi, S. L.; Marque, P. E.; Desmaele, D.; Couvreur, P. A new nanomedicine of gemcitabine displays enhanced anticancer activity in sensitive and resistant leukemia types. *J. Controlled Release* **2007**, *124*, 20–27.

(25) Bildstein, L.; Dubernet, C.; Marsaud, V.; Chacun, H.; Nicolas, V.; Gueutin, C.; Sarasin, A.; Benech, H.; Lepetre-Mouelhi, S.; Desmaele, D.; Couvreur, P. Transmembrane diffusion of gemcitabine

by a nanoparticulate squalenoyl prodrug: an original drug delivery pathway. *J. Controlled Release* **2010**, *147*, 163–170.

(26) Toub, N.; Bertrand, J. R.; Tamaddon, A.; Elhamess, H.; Hillaireau, H.; Maksimenko, A.; Maccario, J.; Malvy, C.; Fattal, E.; Couvreur, P. Efficacy of siRNA nanocapsules targeted against the EWS-Fli1 oncogene in Ewing sarcoma. *Pharm. Res.* **2006**, *23*, 892–900.

(27) Tuschl, T. Expanding small RNA interference. *Nat. Biotechnol.* **2002**, *20*, 446–448.

(28) Ahn, S. H.; Henderson, Y.; Kang, Y.; Chattopadhyay, C.; Holton, P.; Wang, M.; Briggs, K.; Clayman, G. L. An orthotopic model of papillary thyroid carcinoma in athymic nude mice. *Arch. Otolaryngol. Head Neck Surg.* **2008**, *134*, 190–197.

(29) Livak, K. J.; Schmittgen, T. D. Analysis of relative gene expression data using real-time quantitative PCR and the 2(-delta delta C(T)) method. *Methods* **2001**, *25*, 402–408.

(30) Seifeddine, R.; Dreiem, A.; Blanc, E.; Fulchignoni-Lataud, M. C.; Le Frere Belda, M. A.; Lecuru, F.; Mayi, T. H.; Mazure, N.; Favaudon, V.; Massaad, C.; Barouki, R.; Massaad-Massade, L. Hypoxia down-regulates CCAAT/enhancer binding protein-alpha expression in breast cancer cells. *Cancer Res.* **2008**, *68*, 2158–2165.

(31) Seifeddine, R.; Dreiem, A.; Tomkiewicz, C.; Fulchignoni-Lataud, M. C.; Brito, I.; Danan, J. L.; Favaudon, V.; Barouki, R.; Massaad-Massade, L. Hypoxia and estrogen co-operate to regulate gene expression in T-47D human breast cancer cells. *J. Steroid Biochem. Mol. Biol.* **2007**, *104*, 169–179.

(32) Mosmann, T. Rapid colorimetric assay for cellular growth and survival: application to proliferation and cytotoxicity assays. *J. Immunol. Methods* **1983**, *65*, 55–63.